Supporting Information

Re(tBu-bpy)(CO)$_3$Cl supported on multi-walled carbon nanotubes selectively reduces CO_2 in water.

Almagul Zhanaidarova,[a] Simon C. Jones,[b] Emmanuelle Despagnet-Ayoub,[bc] Brian R. Pimentel[d] and Clifford P. Kubiak[ad]

[a.] Department of Materials Science and Engineering, University of California, San Diego. 9500 Gilman Drive, Mail Code 0358, La Jolla, California 92093-0358, United States.

[b.] Electrochemical Technologies Group, Jet Propulsion Laboratory, California Institute of Technology, Pasadena, California 91109, United States.

[c.] Occidental College, Norris Hall of Chemistry, 1600 Campus Rd, Los Angeles, USA

[d.] Department of Chemistry and Biochemistry, University of California, San Diego. 9500 Gilman Drive, Mail Code 0358, La Jolla, California 92093-0358, United States.

Experimental procedures:

Materials: Chemicals were purchased from Sigma Aldrich and Fisher Scientific and used without further purifications. Multi-walled carbon nanotubes (MWCNT) (>98% carbon basis, O.D. x L 6-13 nm x 2.5-20 μm) and graphitized carbon nanofiber (CNF) (iron-free, composed of conical platelets, D x L 100 nm x 20-200 μm) were purchased from Sigma Aldrich. Glassy carbon plates (SA-3, 100 x 100 x t3 mm) were purchased from Tokai Carbon and pre-cut to the area of 1 x 2 cm^2.

Preparation of glassy carbon electrodes. Tokai glassy carbon plates were polished with an alumina slurry (0.05 μm) with subsequent sonication in water, methanol and acetone. Polished glassy carbon plates were connected to a copper wire using an alligator clip and were covered with an epoxy so that the exposed working area of glassy carbon surface was equal to 1 x 1 cm^2.

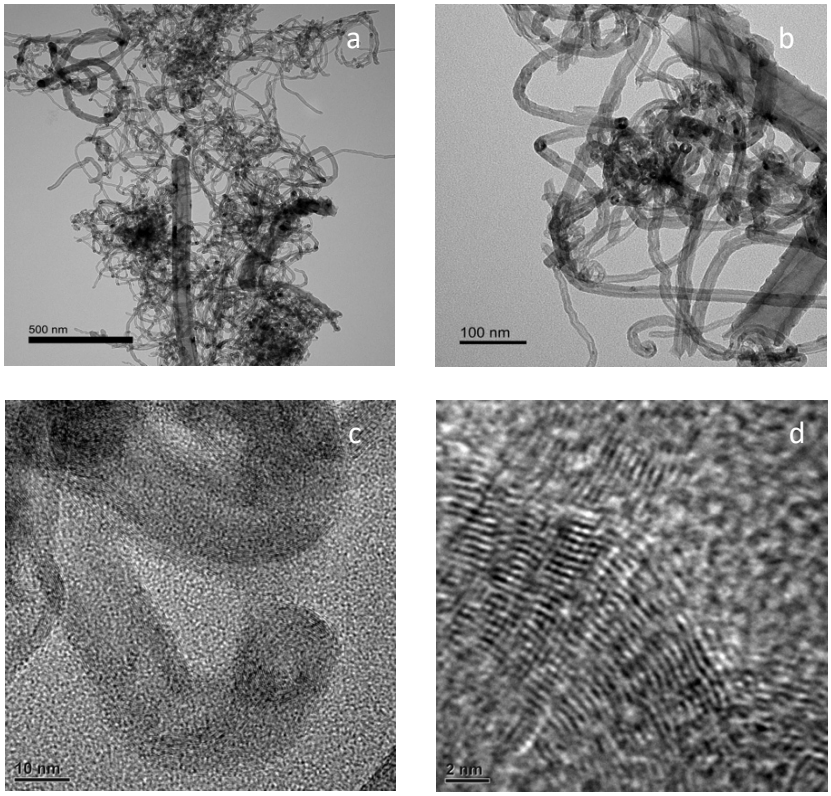

Fig. S1 TEM images of Re(tBu-bpy)/MWCNT - electrode **3** at 25 kX (**a**), 100 kX (**b**), 150 kX (**c**), 690 kX (**d**).

XPS analysis. XPS experiments were performed using a Kratos AXIS-SUPRA instrument equipped with a AL K-alpha monochromatic X-ray source operating at 225W. A pass energy of 160 eV was used for survey spectrum with 1 eV step size and a pass energy of 20 eV was used for details spectra, averaged over 5 scans, with 0.1 eV step size.

Data were analyzed with CASA XPS software. All peaks were referenced to the 1s graphitic carbon peak (284.4 eV)[1] in MWCNT. Peak fittings were performed with a Shirley-type background and Gaussian/Lorentzian line-shapes with 30% Gaussian shape.

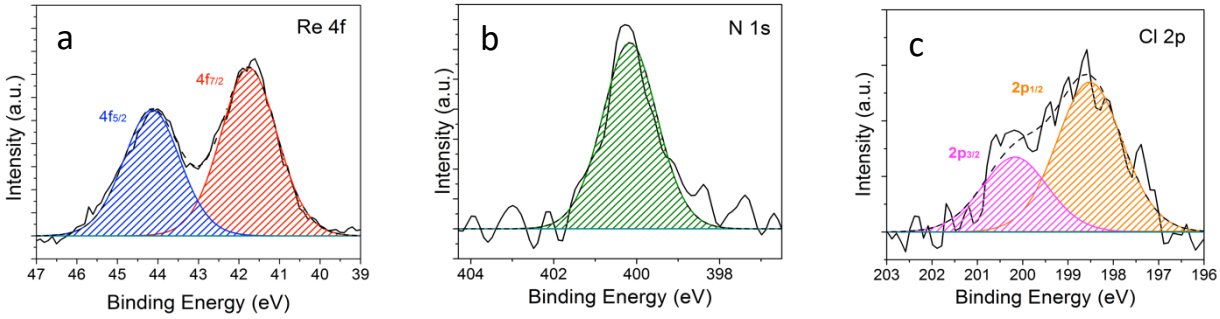

Fig. S2 High-resolution XPS spectra for Re 4f (a), N 1s (b) and Cl 2p (c) of Re(tBu-bpy) on bare GCE.

Table S1. Survey XPS peaks integration.

Re(tBu-bpy)(CO)$_3$Cl/MWCNT	**Re %**	**N %**	**C %**	**O %**	**Cl %**
before CPE	0.98	1.93	93.76	2.45	0.90
after CPE	0.98	1.96	93.63	2.64	0.83
Re(tBu-bpy)/GCE	1.08	2.07	74.49	21.38	0.99

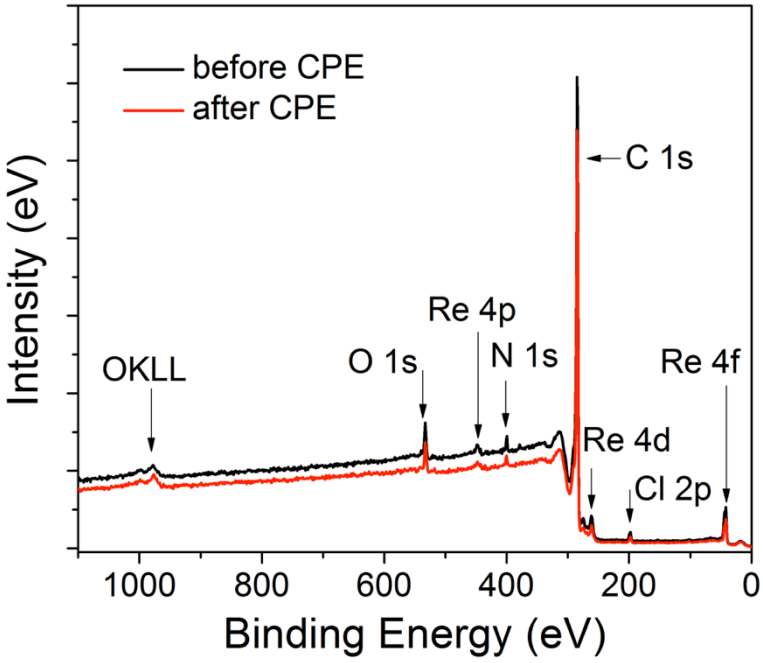

Fig. S3 Survey XPS for Re(tBu-bpy)/MWCNT.

ICP-MS analysis:

Table S2. Results of ICP-MS analysis of Re(tBu-bpy)/MWCNT.

Electrode #	Re(tBu-bpy)/MWCNT mg	Re mg	Re wt %	Re(tBu-bpy) mg	Re(tBu-bpy) wt%
1	7.1	0.01	0.14	0.03	0.42
2	4.8	0.04	0.83	0.10	2.50
3	6.2	0.28	4.52	0.86	13.87
4	6.8	0.51	7.50	1.57	23.08
5	6.6	0.54	8.18	1.66	25.15

Table S3. Summary of electrocatalytic CO_2 reduction using Re(tBu-bpy)/MWCNT electrodes. Electrodes 6-8.

Electrode #	Re(tBu-bpy) (wt %)	Charge (C)	[CO] (μmol)	FE (% CO)	FE (% H_2)	TOF (h^{-1})	I (mA/cm^2)
6 (0.20 mg)*	2.8	7.3	35	94	6	101	2.0
7 (0.30 mg)*	4.1	8.7	44	97	3	83	2.4
8 (0.50 mg)*	6.7	10.2	51	97	3	60	2.9

*TOF calculated based on the total mass of the sample.

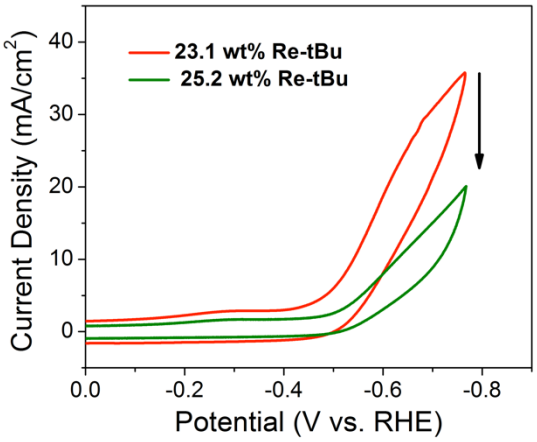

Fig. S4 CV of Re(tBu-bpy)/MWCNT electrodes **4** and **5** in 0.5 M $KHCO_3$ under CO_2. Re(tBu-bpy)/MWCNT electrodes were used as a working, Ag/AgCl as a reference, Pt as a counter electrode. Scan rate 100 mV/s.

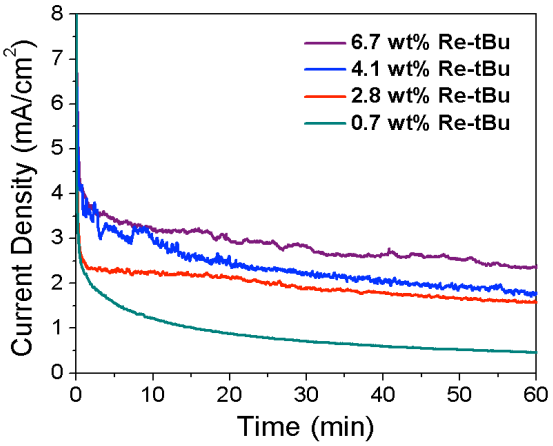

Fig. S5 CPE of Electrodes **1, 6**, **7**, **8** at -0.56 V vs. RHE in CO_2 saturated 0.5 M $KHCO_3$.

Control electrochemical experiments:

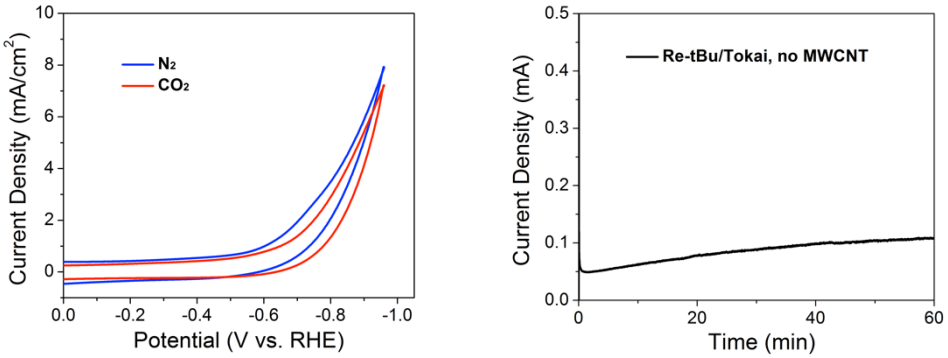

Fig. S6 (left) CV of control Re(tBu-bpy)/GCE in 0.5 M $KHCO_3$ under N_2(blue) and under CO_2 (red). (right) CPE of control Re(tBu-bpy)/GCE in 0.5 M $KHCO_3$ under CO_2 at -0.56 V vs. RHE. FE (H_2) 100%.

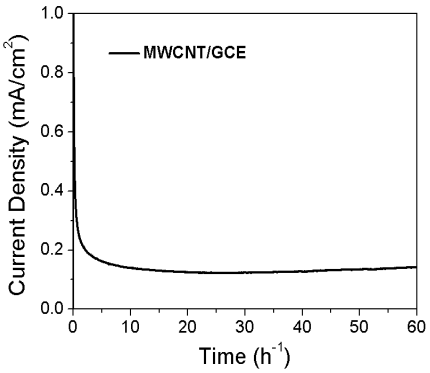

Fig. S7 CPE of blank MWCNT/GCE in 0.5 M $KHCO_3$ under CO_2 at -0.56 V vs. RHE. FE (H_2) = 100 %

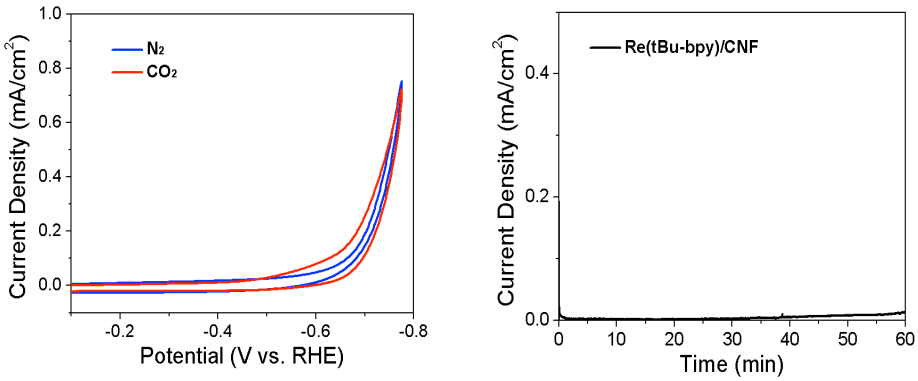

Fig. S8 (left) CV of Re(tBu-bpy)/CNF in 0.5 M $KHCO_3$ under N_2 (blue) and under CO_2 (red). (right) CPE of Re(tBu-bpy)/CNF at -0.56 V vs. RHE in 0.5 M $KHCO_3$ under CO_2 atmosphere.

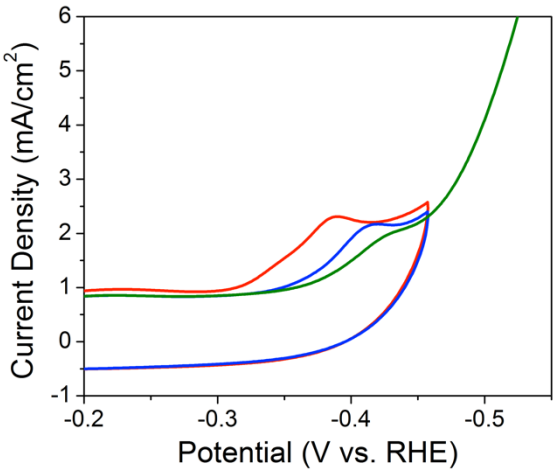

Fig. S9 CV of Re(tBu-bpy)/MWCNT at 25 mV/s in 0.5 M $KHCO_3$ under CO_2 atmosphere. 1st scan (red loine), 2nd scan (blue line), 3rd scan (green line). Electrode **4** was used as a working electrode, Ag/AgCl as a reference, Pt as a counter electrode. Scan rate 25 mV/s.

Charge Q was calculated using the area under the curve per scan rate and moles of electroactive catalyst was calculated according to Equation: $\Gamma = Q/nFA$, where n is the number electrons (n = 1), F is the Faraday constant, and A is the area of the electrode.

Table S4. Electroactive species obtained from CV and corresponding CPE current.

Electrode #	**Mol_{EA} (x10^{-8})**	**Current Density (mA/cm^2)**
1	0.68	1.0
2	0.79	1.3
3	1.1	3.1
4	1.3	4.0
5	0.82	2.1

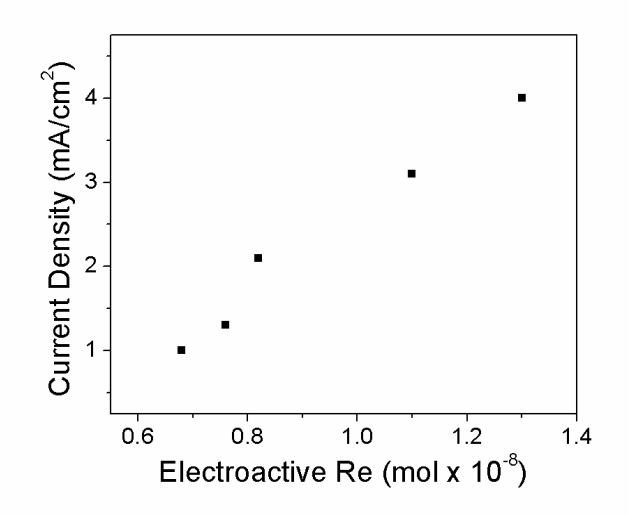

Fig. S10 Linear relationship of CPE current vs. EA rhenium.

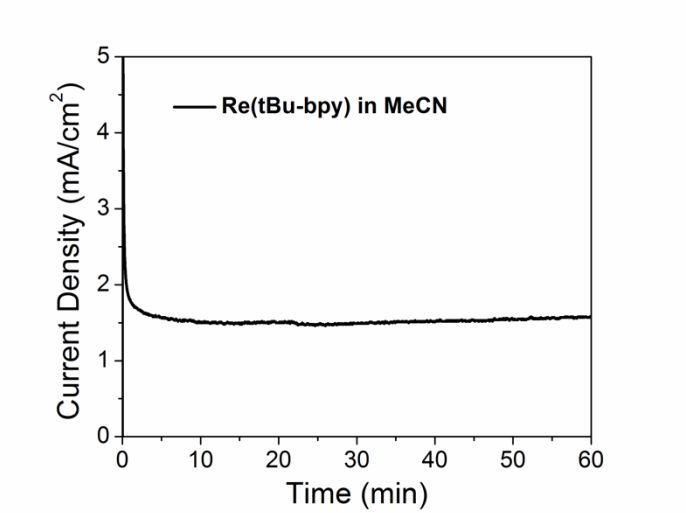

Fig. S11 CPE of 0.1 mM Re(tBu-bpy)$(CO)_3Cl$ at -2.1 V vs. $Fc^{+/0}$ in in CO_2 saturated MeCN / 0.5 H_2O solution. 0.1 M $TBAPF_6$ was used as electrolyte. Bare MWCNT/CNF/GCE was used as a working electrode, Ag/AgCl as a reference, Pt as a counter electrode.

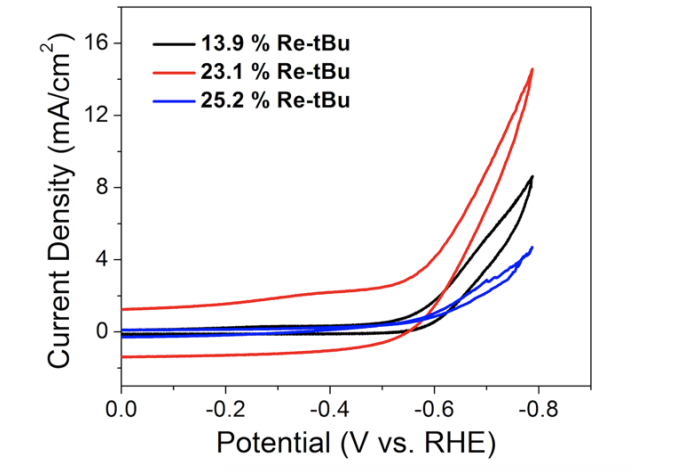

Fig. S12 CV of Re(tBu-bpy)/MWCNT in CO_2 saturated 0.1 M $KHCO_3$. Electrodes 2, 3, 4 were used as working electrodes, Ag/AgCl as a reference, Pt as a counter electrode. Scan rate 100mV/s.

Gas adsorption measurements. Materials were characterized by N_2 physisorption at 77 K (Micromeritics ASAP 2020) after a 12 h activation under vacuum at 423 K. Brunauer-Emmet-Teller (BET) surface areas were calculated following established consistency criterion.[2] The composite sample without rhenium demonstrates a comparable surface area to other reported MWCNTs[3-7], although literature values vary greatly. Increasing loading of the rhenium complex results in surface area loss in excess of the added non-porous mass (Table S5), indicating surface adsorption.

Table S5. Results of gas adsorption measurements.

Sample	BET Surface Area (m^2/g)
Blank	175 ± 0.6
1.4% Re	120 ± 0.4
12.5% Re	107 ± 0.9
22.2 %	87 ± 0.9
23.4 %	83 ± 0.8

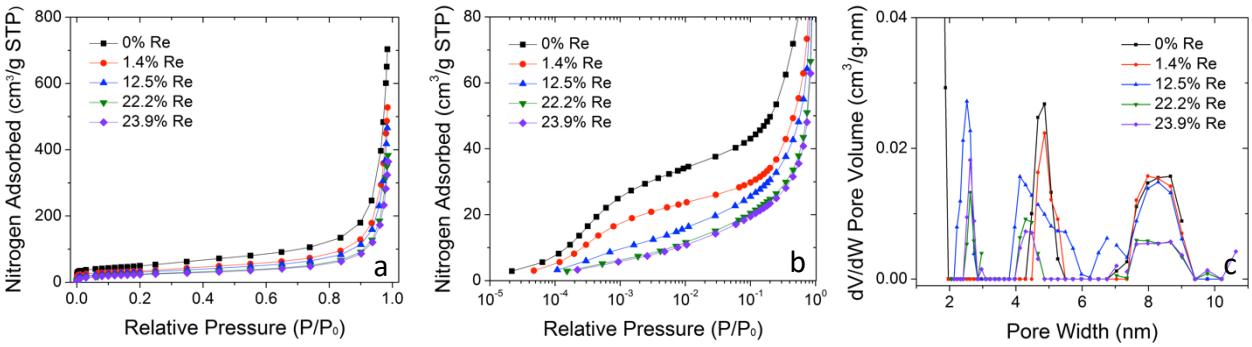

Fig. S13 N_2 adsorption isotherms (77 K) of Re-loaded MWCNT/CNF composites in (**a**) linear and (**b**) log scale; (**c**) DFT pore size distributions of samples calculated from N_2 isotherms (77 K).

Sample pore size distributions (PSD) were calculated using the Microactive software package (Micromeritics) as multiwalled nanotubes under the DFT Pore Size model (Fig. S4c).

The PSD of the blank sample shows a bimodal pore size distribution up to 10 nm—pore volume beyond this point is poorly defined and likely a result of interparticle condensation rather than intrinsic material porosity—which is closely mimicked by samples with low (1.4%) rhenium loading. Intermediate rhenium loadings (12.5%) result in noticeable changes in the PSD, where new pore distributions appear near 2.5 nm and 7 nm, likely from the disruption of the larger parent distributions. Moreover, the previously well-defined distribution at 5 nm is noticeably broadened. Further increasing (>20%) rhenium content continues to disrupt the pristine PSD, with a pronounced loss of cumulative porosity throughout the distribution. The changes in PSD in conjunction with the decreases in BET surface area suggest that the rhenium complex is located within the pores of the substrate, though it is not possible to rule out the presence of external complex adsorption.

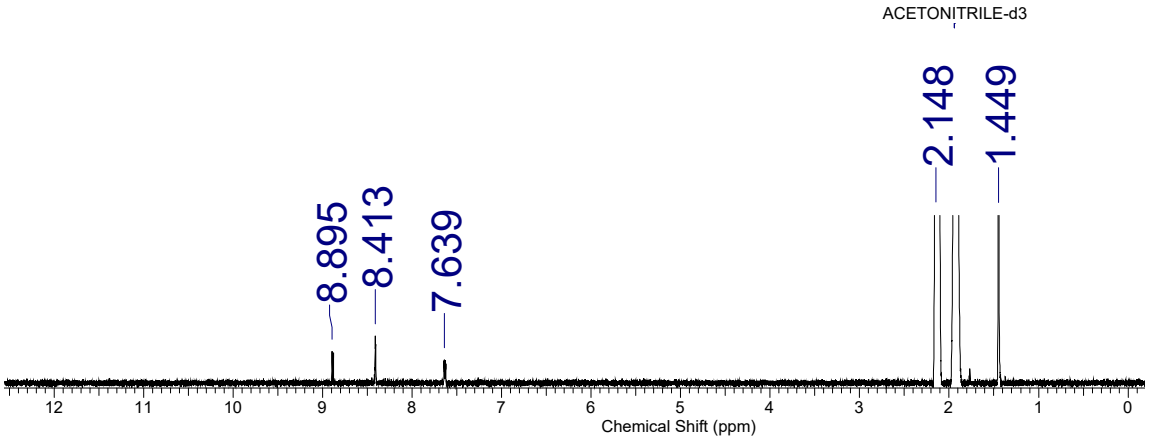

Fig. S14 ^{1}H NMR of Re(tBu-bpy)/MWCNT electrode soaked in CD_3CN.

^{1}H NMR. To analyze the composition of electrodes after CPE samples were soaked in deuterated acetonitrile and analyzed via ^{1}H NMR spectroscopy. Chemical shifts corresponding to bipyridine ligand were detected and matched with the spectra of Re(tBu-bpy)$(CO)_3Cl$.[8] ^{1}H NMR (400 MHz, CD_3CN): δ 1.45 (s, 18H, tBu), 7.64 (dd, 2H), 8.41 (d, 2H), 8.88 (d, 2H).

Solution IR. The IR experiments of the electrodes soaked in MeCN showed IR peaks υ(CO) 2023, 1916, 1898 cm^{-1} and matched with the IR spectra of Re(tBu-bpy)$(CO)_3Cl$.

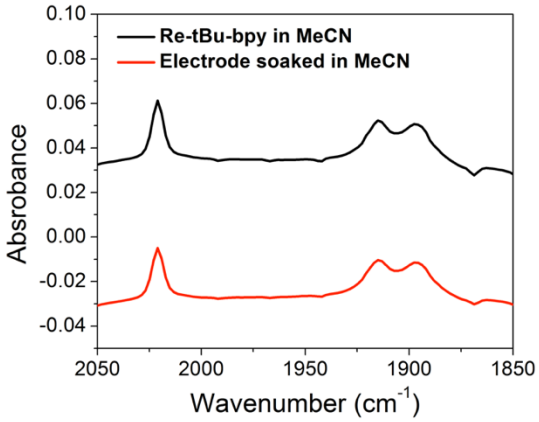

Fig. S15 IR spectra of Re(tBu-bpy)$(CO)_3Cl$ (black) dissolved in MeCN and Re(tBu-bpy)/MWCNT dissolved in MeCN (red).

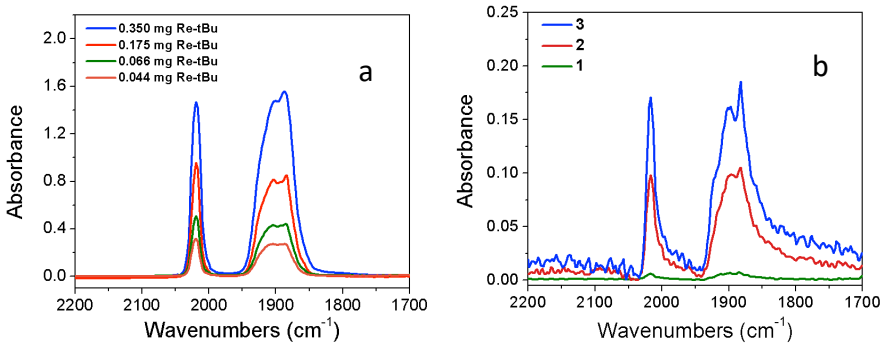

Fig. S16 (a) Calibration: IR spectra of Re(tBu-bpy)(CO)$_3$Cl in KBr pellet, (b) IR spectra of Re-(tBu-bpy)/MWCNT in KBr pellet collected from electrode **2** (green), electrode **3** (red) and electrode **4** (blue).

KBr pellet IR. A sample of Re(tBu-bpy)(CO)$_3$Cl of a known mass was pressed into a pellet with KBr salt and was analyzed using infrared spectroscopy. The IR spectra showed CO peaks at υ(CO) 2017, 1903, 1884 cm^{-1}. These pellets with four known concentrations were used as a standard to plot a calibration line for the future measurements (Fig. S16a). The solid samples of Re(tBu-bpy)/MWCNT with various Re(tBu-bpy)(CO)$_3$Cl loadings were pressed into KBr pellets to perform IR experiments of Re(tBu-bpy)(CO)$_3$Cl adsorbed on MWCNTs. These samples were prepared by mixing electrode materials scraped from the electrode surface with a surgical blade with dry KBr salt. The IR spectra of these samples matched with a standard and showed three CO stretches at 2019, 1900, 1884 cm^{-1} (Fig. S16b). Catalyst concentrations for three different Re(tBu-bpy)/MWCNT samples were calculated and are listed in Table S6, Table S7.

Table S6. IR data of Re(tBu-bpy)(CO)$_3$Cl in KBr pellet.

Adsorption			**Extinction coefficient**			**Mass (mg)**
1884	**1903**	**2019**	**E 1884**	**E 1898**	**E 2019**	
1.556	1.478	1.467	19.142	18.182	18.047	0.350
0.837	0.811	0.821	20.593	19.954	20.200	0.175
0.429	0.420	0.458	21.110	20.667	22.537	0.088

0.250	0.266	0.270	21.870	26.179	23.620	0.044
			20.679	21.245	21.101	

Table S7. IR data of Re(tBu-bpy)$(CO)_3$Cl/MWCNT in KBr pellet.

Adsorption			Extinction coefficient			Mass (mg)
1884	**1903**	**2019**	**E 1884**	**E 1898**	**E 2019**	
0.008	0.007	0.008	20.68	21.25	21.10	0.06
0.11	0.098	0.098	20.68	21.25	21.10	0.84
0.19	0.17	0.18	20.68	21.25	21.10	1.77

Table S8. CPE data for the 7-hour experiment in CO_2 saturated 0.5 M $KHCO_3$.

		Gc area		mol CO		current efficiency %				TON	TOF (h-1)
time (h)	Coulombs	H_2	CO	H_2	CO	H_2	CO	total	Electrons	mol CO/molCat	
0.5	9.00	1.68	220.00	5.46E-07	4.60E-05	1.2%	99.4%	100.5%	9.33E-05	16.94	33.89
1.0	14.00	2.14	356.00	6.68E-07	7.20E-05	1.0%	99.2%	100.2%	1.45E-04	26.32	26.32
1.5	18.00	3.11	481.00	9.30E-07	9.30E-05	1.0%	99.9%	100.9%	1.87E-04	34.08	22.72
2.0	23.00	3.78	624.00	1.11E-06	1.18E-04	0.9%	99.3%	100.2%	2.38E-04	43.25	21.63
2.5	28.00	4.53	716.00	1.38E-06	1.42E-04	1.0%	97.7%	98.7%	2.90E-04	51.84	20.73
3.0	33.00	5.55	826.00	1.73E-06	1.67E-04	1.0%	97.7%	98.7%	3.42E-04	61.07	20.36
3.5	36.00	6.48	929.00	1.98E-06	1.84E-04	1.1%	98.6%	99.7%	3.73E-04	67.26	19.22
4.0	39.70	7.24	1025.00	2.21E-06	2.03E-04	1.1%	98.7%	99.8%	4.11E-04	74.21	18.55
4.5	43.30	8.12	1104.00	2.54E-06	2.23E-04	1.1%	99.5%	100.6%	4.49E-04	81.63	18.14
5.0	46.60	8.82	1218.00	2.70E-06	2.41E-04	1.1%	99.9%	101.0%	4.83E-04	88.18	17.64
5.5	49.70	9.75	1298.00	2.98E-06	2.57E-04	1.2%	99.8%	101.0%	5.15E-04	93.97	17.09
6.0	52.80	10.44	1365.00	3.19E-06	2.70E-04	1.2%	98.8%	100.0%	5.47E-04	98.82	16.47
6.5	55.70	11.48	1445.00	3.51E-06	2.86E-04	1.2%	99.1%	100.3%	5.77E-04	104.61	16.09
7.0	58.40	12.50	1523.00	3.82E-06	3.02E-04	1.2%	99.0%	100.2%	6.05E-04	110.26	15.75

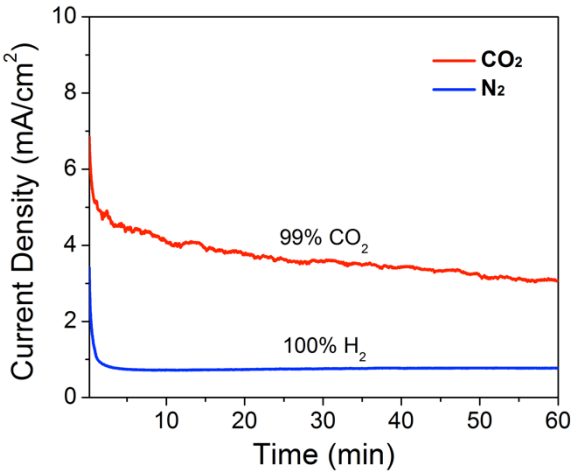

Fig. S17 CPE of Electrode 4 under N_2 (blue) vs. CO_2 (red). At -0.56 V vs. RHE in 0.5 M $KHCO_3$.

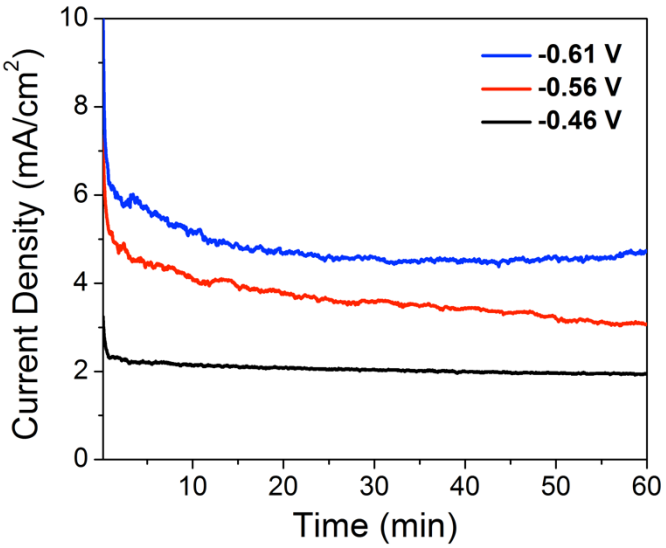

Fig. S18 CPE of Electrode 4 at -0.46, -0.56, -0.61 V vs. RHE in CO_2 saturated 0.5 M $KHCO_3$.

References:

1. Susi T.; Pichler T.; Ayala P.*, Beilstein J. Nanotechnol. ,* 2015, ***6***, 177-192.
2. Walton K. S.; Snurr R. Q.*, J. Am. Chem. Soc.,* 2007, ***129***, 8552-8556.
3. Liu, B.; Li, Z.; Xu, S.; Han, D.; Lu, D.*„ j. Alloys Compd. ,* 2014, 19-24.
4. Solhy, A.; Machado, B. F.; Beausoleil, J.; Kihn, Y.; Gonçalves, F.; Pereira, M. F. R.; Órfão, J. J. M.; Figueiredo, J. L.; Faria, J. L.; Serp, P.*„ Carbon,* 2008, 1194-1207.
5. Yang, C.; Hu, X.; Wang, D.; Dai, C.; Zhang, L.; Jin, H.; Agathopoulos, S.*„ J. Power Sources,* 2006, ***160***, 187-193.
6. Kim, S. D.; Kim, J. W.; Im, J. S.; Kim, Y. H.; Lee, Y. S.*„ J. Fluorine Chem.,* 2007, ***128***, 60-64.
7. Wang, W.; Serp, P.; Kalck, P.; Silva, C. G.; Faria, J. L.*„ Materl. Res. Bull.,* 2008, ***43***.
8. Smieja J. M.; Kubiak C. P.*, Inorg. Chem.,* 2010, ***49***, 9283-9289.